Electronic Supplementary Material (ESI) for Physical Chemistry Chemical Physics.

Electronic Supplementary Information

A cationic naphthyl derivative defies the Non Equilibrated Excited Rotamers principle

A. Cesaretti, B. Carlotti, F. Elisei, C.G. Fortuna, G. Consiglio and A. Spalletti

Spectral behaviour

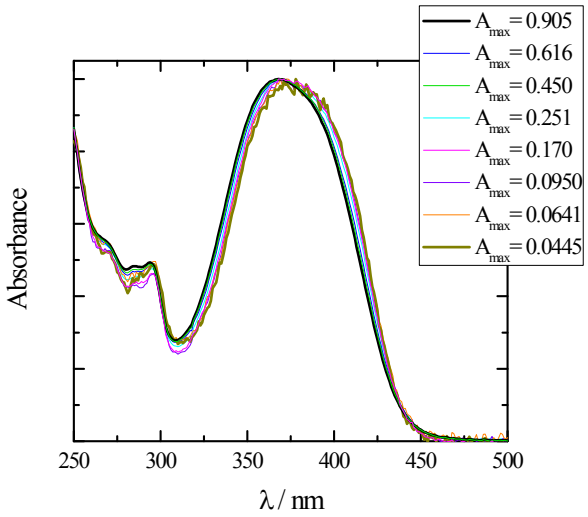

Figure 1S. Concentration effect on the absorption spectrum of **2-N** in DCM.

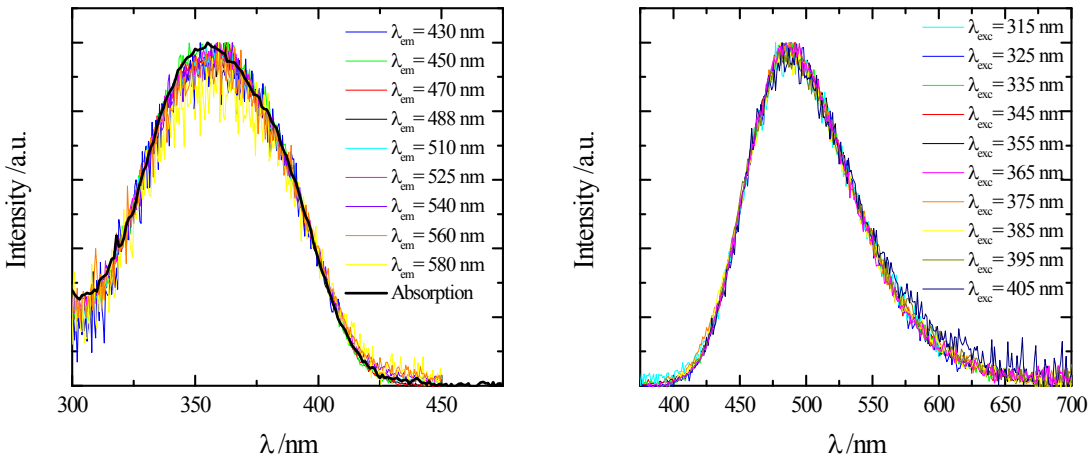

Figure 2S. Emission wavelength effect on the excitation spectrum (left graph, with λ_{em}= 430–580 nm, the absorption is reported for comparison in thick black line) and excitation wavelength effect on the emission spectrum (right graph, with λ_{exc}= 315–405 nm) for **2-N** in MeOH at room temperature.

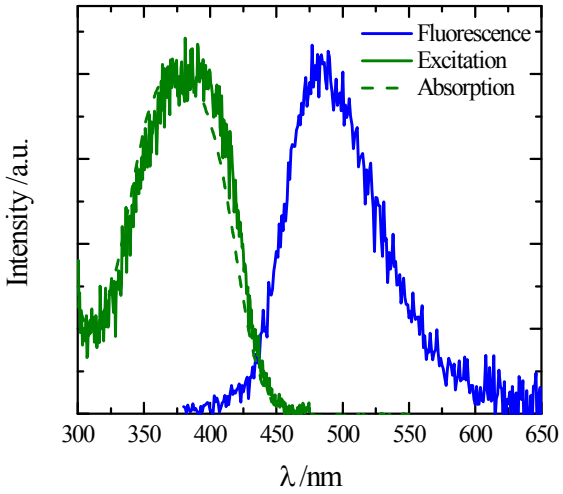

Figure 3S. Absorption (olive dashed line), excitation (olive solid line) and emission (blue solid line) spectra of **2-N** in dilute DCM at room temperature.

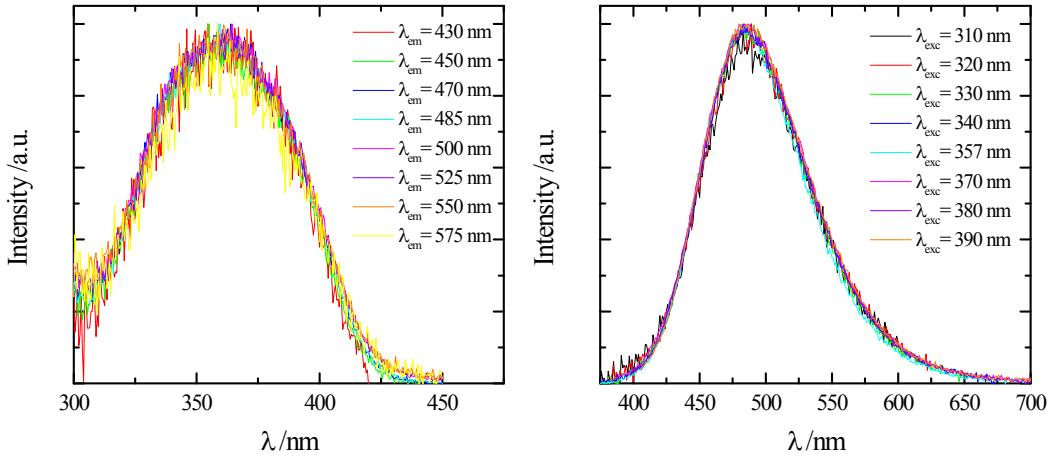

Figure 4S. Emission wavelength effect on the excitation spectrum (left graph, with λ_{em}= 430–575 nm) and excitation wavelength effect on the emission spectrum (right graph, with λ_{exc}= 310–390 nm) for **2-N** in EtGly at room temperature.

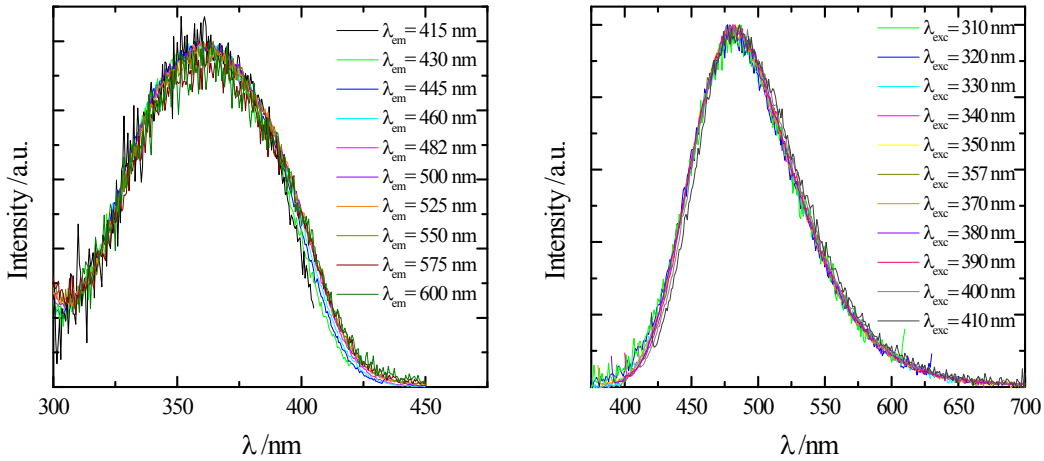

Figure 5S. Emission wavelength effect on the excitation spectrum (left graph, with λ_{em}= 415–600 nm) and excitation wavelength effect on the emission spectrum (right graph, with λ_{exc}= 310–410 nm) for **2-N** in MeOH/Gly 50/50 at room temperature.

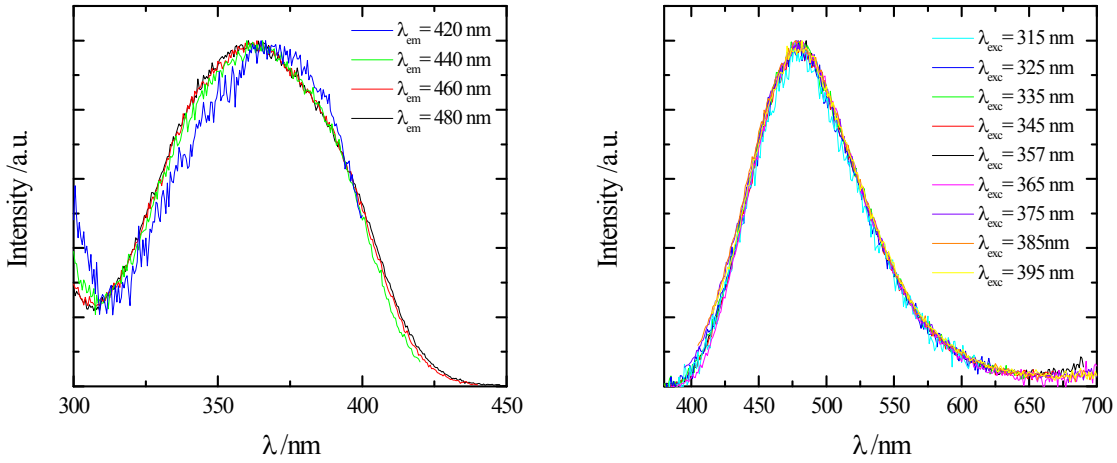

Figure 6S. Emission wavelength effect on the excitation spectrum (left graph, with λ_{em}= 420–480 nm) and excitation wavelength effect on the emission spectrum (right graph, with λ_{exc}= 315–395 nm) for **2-N** in MeOH/Gly 20/80 at room temperature.

Quantum-mechanical calculations

Table 1S. Theoretical absorption and emission wavelengths of **2-N** (rotamers A, B, C and D), oscillator strengths, nature and composition in terms of molecular orbitals obtained by the CAM-B3LYP/6-31+G(d) model in DCM (CPCM), together with the experimental absorption maxima.

A rotamer					
Transition	**λ_{th}/nm**	**f**	**MO**	**c_i^2/%**	**λ_{exp}/nm**
$S_0 \rightarrow S_1$	374	1.3315	$\pi_H \rightarrow \pi_L^*$	80	370
$S_0 \rightarrow S_2$	315	0.1475	$\pi_{H-1} \rightarrow \pi_L^*$	67	
$S_0 \rightarrow S_3$	275	0.1699	$\pi_H \rightarrow \pi_{L+2}^*$	50	
$S_0 \rightarrow S_4$	262	0.2986	$\pi_H \rightarrow \pi_{L+1}^*$	36	
$S_0 \rightarrow S_5$	246	0.1486	$\pi_{H-1} \rightarrow \pi_{L+2}^*$	39	
$S_0 \rightarrow S_6$	238	0.0567	$\pi_{H-2} \rightarrow \pi_L^*$	55	
$S_0 \rightarrow S_7$	226	0.7590	$\pi_H \rightarrow \pi_{L+3}^*$	42	
$S_0 \rightarrow S_8$	218	0.0219	$\pi_{H-1} \rightarrow \pi_{L+1}^*$	27	
$S_0 \rightarrow S_9$	214	0.0265	$\pi_{H-3} \rightarrow \pi_L^*$	49	
$S_0 \rightarrow S_{10}$	276	0.1043	$\pi_{H-4} \rightarrow \pi_L^*$	27	
$S_1 \rightarrow S_0$	458	1.6002	$\pi_H \rightarrow \pi_L^*$	93	
B rotamer					
$S_0 \rightarrow S_1$	383	1.0556	$\pi_H \rightarrow \pi_L^*$	81	370
$S_0 \rightarrow S_2$	321	0.2933	$\pi_{H-1} \rightarrow \pi_L^*$	70	
$S_0 \rightarrow S_3$	281	0.0965	$\pi_H \rightarrow \pi_{L+2}^*$	35	
$S_0 \rightarrow S_4$	260	0.4449	$\pi_H \rightarrow \pi_{L+1}^*$	33	
$S_0 \rightarrow S_5$	247	0.0344	$\pi_{H-1} \rightarrow \pi_{L+2}^*$	20	
$S_0 \rightarrow S_6$	237	0.0041	$\pi_{H-2} \rightarrow \pi_L^*$	50	
$S_0 \rightarrow S_7$	227	0.6508	$\pi_{H-1} \rightarrow \pi_{L+2}^*$	38	
$S_0 \rightarrow S_8$	218	0.0769	$\pi_{H-3} \rightarrow \pi_L^*$	42	
$S_0 \rightarrow S_9$	216	0.0420	$\pi_{H-1} \rightarrow \pi_{L+1}^*$	33	
$S_0 \rightarrow S_{10}$	211	0.3045	$\pi_{H-4} \rightarrow \pi_{L+6}^*$	61	
$S_1 \rightarrow S_0$	473	1.2558	$\pi_H \rightarrow \pi_L^*$	94	
C rotamer					
$S_0 \rightarrow S_1$	390	1.4834	$\pi_H \rightarrow \pi_L^*$	84	370
$S_0 \rightarrow S_2$	324	0.1374	$\pi_{H-1} \rightarrow \pi_L^*$	75	
$S_0 \rightarrow S_3$	276	0.0314	$\pi_H \rightarrow \pi_{L+1}^*$	34	
$S_0 \rightarrow S_4$	269	0.2390	$\pi_H \rightarrow \pi_{L+2}^*$	46	
$S_0 \rightarrow S_5$	245	0.1577	$\pi_{H-1} \rightarrow \pi_{L+2}^*$	53	
$S_0 \rightarrow S_6$	241	0.0257	$\pi_{H-2} \rightarrow \pi_L^*$	67	
$S_0 \rightarrow S_7$	224	0.8232	$\pi_{H-1} \rightarrow \pi_{L+2}^*$	32	
$S_0 \rightarrow S_8$	218	0.0237	$\pi_{H-3} \rightarrow \pi_L^*$	53	
$S_0 \rightarrow S_9$	216	0.0790	$\pi_{H-1} \rightarrow \pi_{L+1}^*$	35	
$S_0 \rightarrow S_{10}$	208	0.2109	$\pi_{H-4} \rightarrow \pi_L^*$	39	
$S_1 \rightarrow S_0$	460	1.6231	$\pi_H \rightarrow \pi_L^*$	94	
D rotamer					
$S_0 \rightarrow S_1$	389	1.1036	$\pi_H \rightarrow \pi_L^*$	83	370
$S_0 \rightarrow S_2$	324	0.3128	$\pi_{H-1} \rightarrow \pi_L^*$	73	

$S_0 \rightarrow S_3$	282	0.1822	$\pi_H \rightarrow \pi_{L+1}^*$	41	
$S_0 \rightarrow S_4$	264	0.2779	$\pi_H \rightarrow \pi_{L+2}^*$	42	
$S_0 \rightarrow S_5$	245	0.0581	$\pi_{H-1} \rightarrow \pi_{L+2}^*$	23	
$S_0 \rightarrow S_6$	239	0.0224	$\pi_{H-2} \rightarrow \pi_L^*$	50	
$S_0 \rightarrow S_7$	225	0.6072	$\pi_H \rightarrow \pi_{L+3}^*$	42	
$S_0 \rightarrow S_8$	219	0.0123	$\pi_{H-1} \rightarrow \pi_{L+1}^*$	19	
$S_0 \rightarrow S_9$	218	0.0298	$\pi_{H-3} \rightarrow \pi_L^*$	54	
$S_0 \rightarrow S_{10}$	210	0.2356	$\pi_H \rightarrow \pi_{L+6}^*$	72	
$S_1 \rightarrow S_0$	478	1.2542	$\pi_H \rightarrow \pi_L^*$	95	488

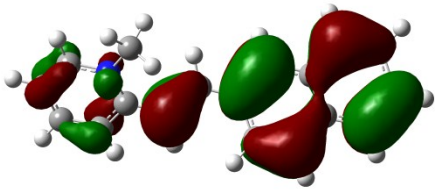
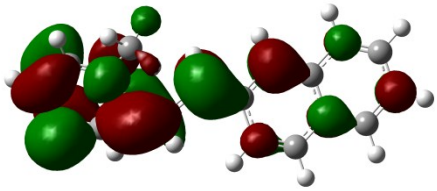

A rotamer: HOMO LUMO

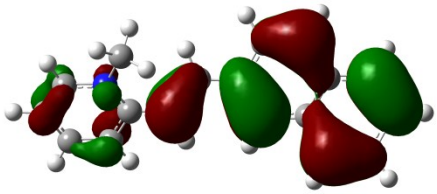
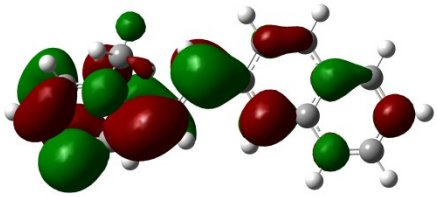

B rotamer: HOMO LUMO

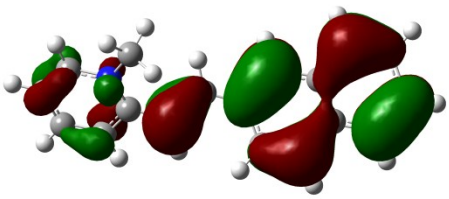
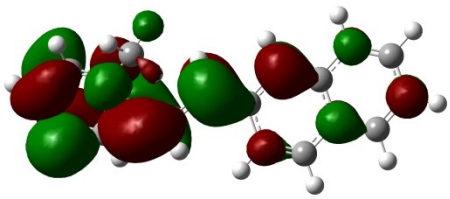

C rotamer HOMO LUMO

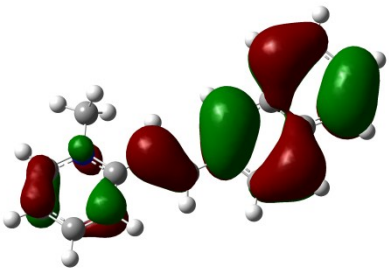
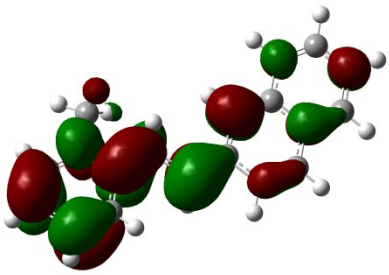

D rotamer HOMO LUMO

Chart 2S. Molecular orbitals of **2-N** (rotamers A-D) obtained by the CAM-B3LYP/6-31+G(d) model.

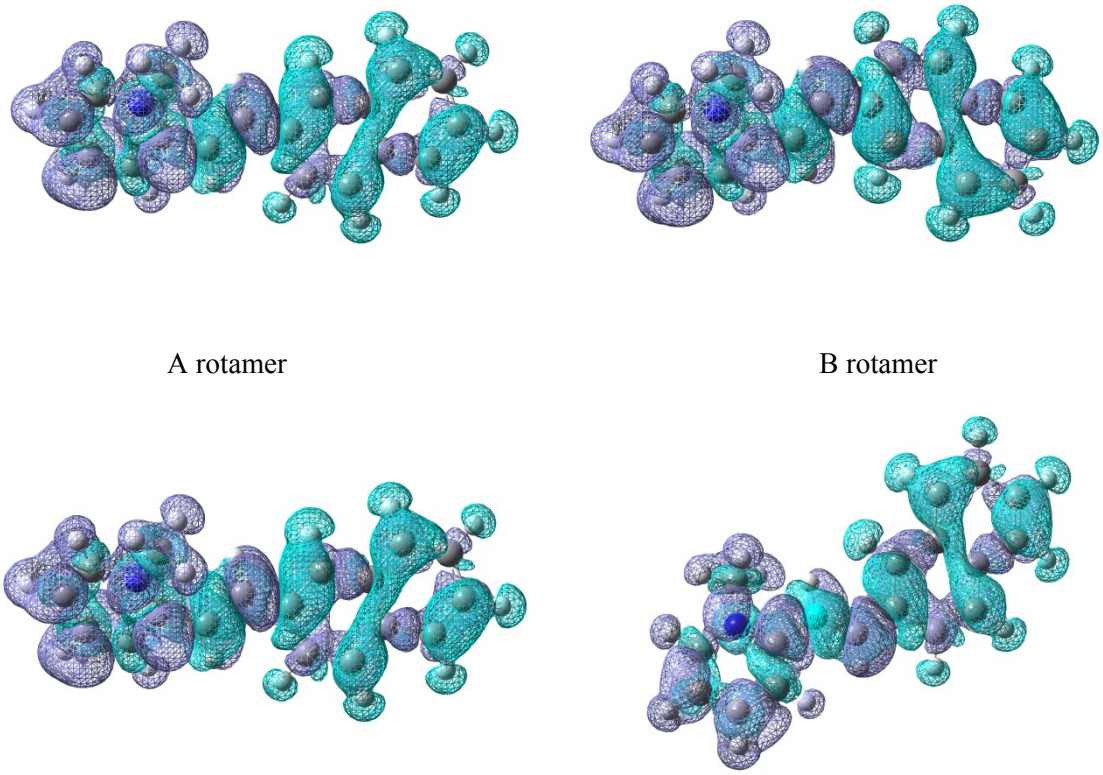

A rotamer B rotamer

C rotamer D rotamer

Chart 3S. Effect of the $S_0 \rightarrow S_1$ transition on the electron density of **2-N** (rotamers A-D); increase and decrease of electron densities are represented by violet and cyano, respectively.

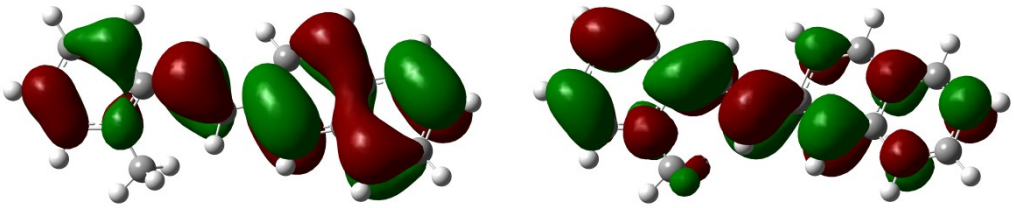

A rotamer HOMO LUMO

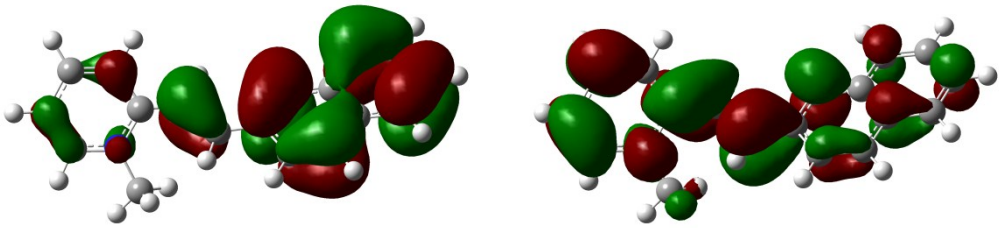

B rotamer HOMO LUMO

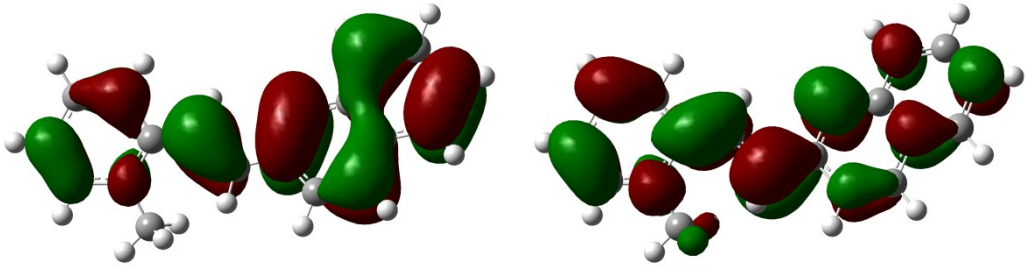

C rotamer HOMO LUMO

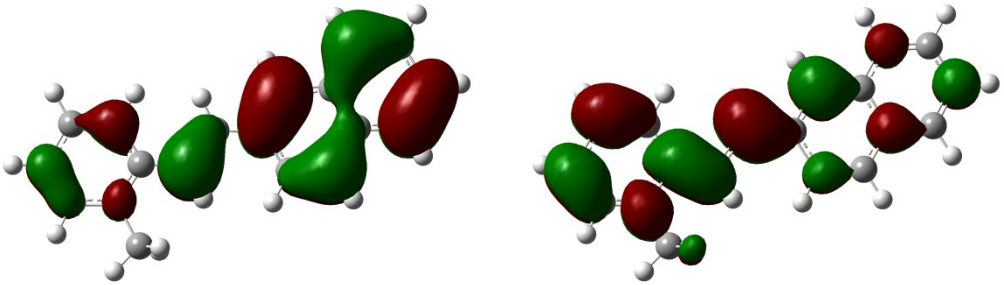

HOMO LUMO

D rotamer

Chart 4S. Molecular orbitals of **2-N** (rotamers A-D) @$S_{1,rel}$ obtained by the CAM-B3LYP/6-31+G(d) model.

Table 2S. Dipole moments and main dihedral angles (Deg) of **2-N** rotamers obtained by the CAM-B3LYP/6-31+G(d) model in DCM (CPCM).

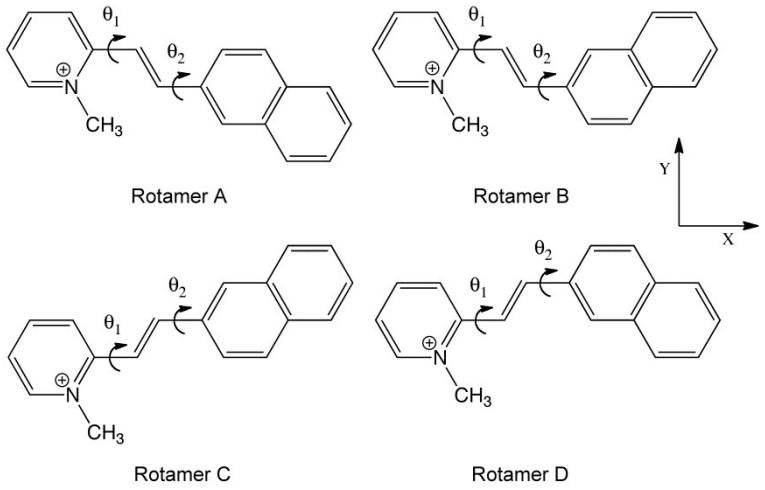

rotamer	state	$\|\mu_x\|$	$\|\mu_y\|$	$\|\mu_z\|$	$\|\mu_T\|$	θ_1	θ_2
A	S_0	15.9	1.93	0.39	15.0	34.5	9.0
	$S_{1,FC}$	3.63	1.88	0.49	4.12		
	$S_{1,rel}$	4.61	1.90	0.28	4.99	11.6	4.2
B	S_0	15.2	0.81	0.69	15.2	33.7	9.4
	$S_{1,FC}$	4.14	0.99	0.77	4.33		
	$S_{1,rel}$	5.08	0.84	0.45	5.17	11.9	4.0
C	S_0	14.8	0.78	0.00	14.9	0.1	0.0
	$S_{1,FC}$	5.13	1.21	0.00	5.27		
	$S_{1,rel}$	5.78	1.12	0.00	5.88	0.0	0.0
D	S_0	14.7	2.05	0.34	14.9	22.0	2.8
	$S_{1,FC}$	4.65	2.30	0.36	5.20		
	$S_{1,rel}$	5.46	2.30	0.00	5.93	0.0	0.0

Ultrafast measurements

Table 3S. Spectral and kinetic properties of **2-N** obtained from femtosecond excited state absorption measurements in solvents of different polarity and/or viscosity.

	2-N		
Solvent	**τ /ps**	**λ /nm**	**Assignment**
DCM	0.62	575(+), 720(+)^{sh}	Solv.
	14	450(+), 495(–) 555(+), 715(+)^{sh}	VC o CR
	85	455(+), 500(–), 545(+), 720(+)^{sh}	$S_{1,rel}$(D)
	rest	broad	T_1
DCE	0.25	525(+), 580(+)	Solv.
	3.1	490(–), 565(+), 715(+)^{sh}	Solv.
	63	500(–), 545(+), 685(+)	$S_{1,rel}$(D)
	rest	broad	T_1
MeCN	0.50	570(+)	Solv.
	4.8	500(–), 540(+), 590(–), 710(+)	VC o CR
	82	495(–), 530(+), 590(–), 720(+)	$S_{1,rel}$(D)
2-PrOH	0.69	515(–), 545(+)^{sh}, 605(+), 690(+)^{sh}	Solv.
	8.4	490(–), 570(+), 690(+)^{sh}	Solv.
	82	490(–), 555(+), 685(+)	$S_{1,rel}$(D)
EtOH	0.40	520(+)^{sh}, 580(+)	Solv.
	8.1	480(−), 560(+)	Solv.
	78	495(−), 540(+), 720(+)	$S_{1,rel}$(D)
MeOH	0.40	570(+)	Solv.
	3.5	490(−), 555(+)	Solv.
	85	500(–), 540(+), 580(–), 710(+)	$S_{1,rel}$(D)
	rest	broad	T_1
MeOH/Gly 50:50	0.68	525(+), 570(+), 700(+)^{sh}	Solv.
	10	485(−), 560(+), 680(+)^{sh}	Solv.
	100	495(–), 545(+), 590(–), 690(+)	$S_{1,rel}$(D)
	rest	broad	T_1
EtGly	0.77	535(+), 575(+), 705(+)^{sh}	Solv.
	28	<495(−), 560(+), 700(+)^{sh}	Solv.
	118	<510(−), 550(+), 590(–), 675(+)^{sh}	$S_{1,rel}$(D)
	rest	broad	T_1
W/EtOH 70:30	0.06	485(–), 565(+), 690(+)^{sh}	Solv.
	1.7	485(−), 555(+)	Solv.
	74	495(−), 540(+), 700(+)	$S_{1,rel}$(D)

Temperature effect on the absorption and emission

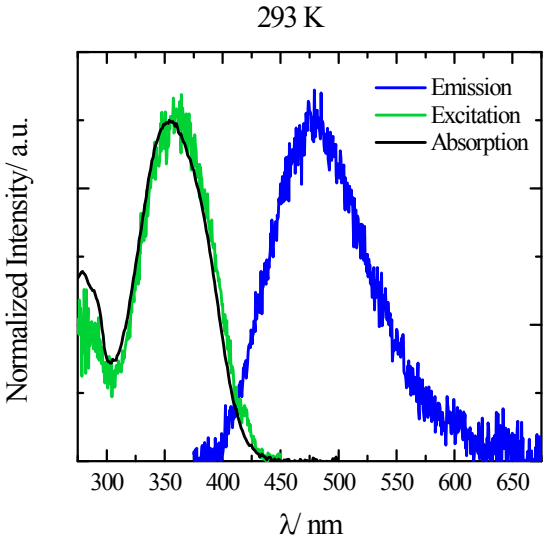

Figure 7S. Absorption (black line), excitation (green line) and emission (blue line) spectra of **2-N** in EPA at room temperature.

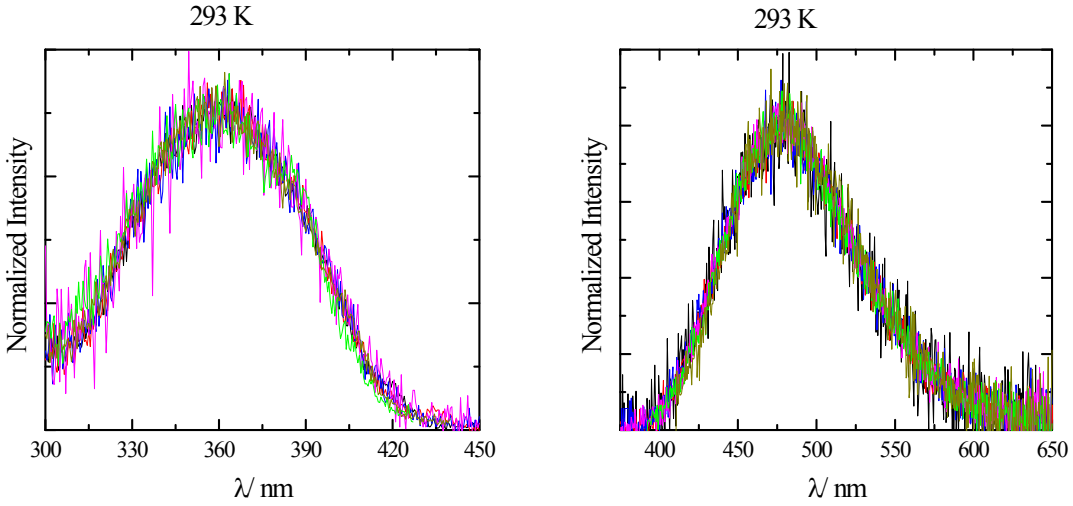

Figure 8S. Emission wavelength effect on the excitation spectrum (left graph, with λ_{em}= 420–480 nm) and excitation wavelength effect on the emission spectrum (right graph, with λ_{exc}= 325–400 nm) for **2-N** in EPA at room temperature.

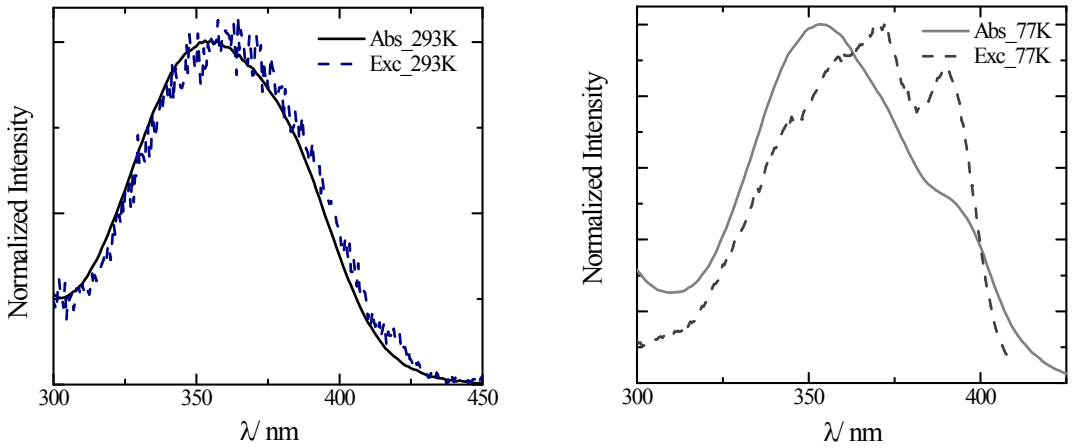

Figure 9S. Absorption and excitation spectra at 293 K (λ_{em} = 480 nm, left graph) and 77 K (λ_{em} = 430 nm, right graph) for **2-N** in EPA.

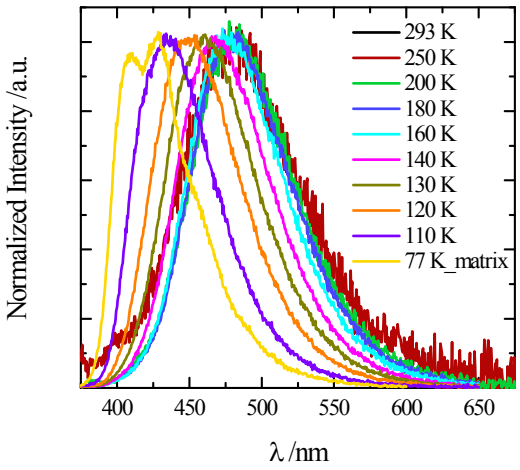

Figure 10S. Temperature effect on the emission spectra of **2-N** in EPA.

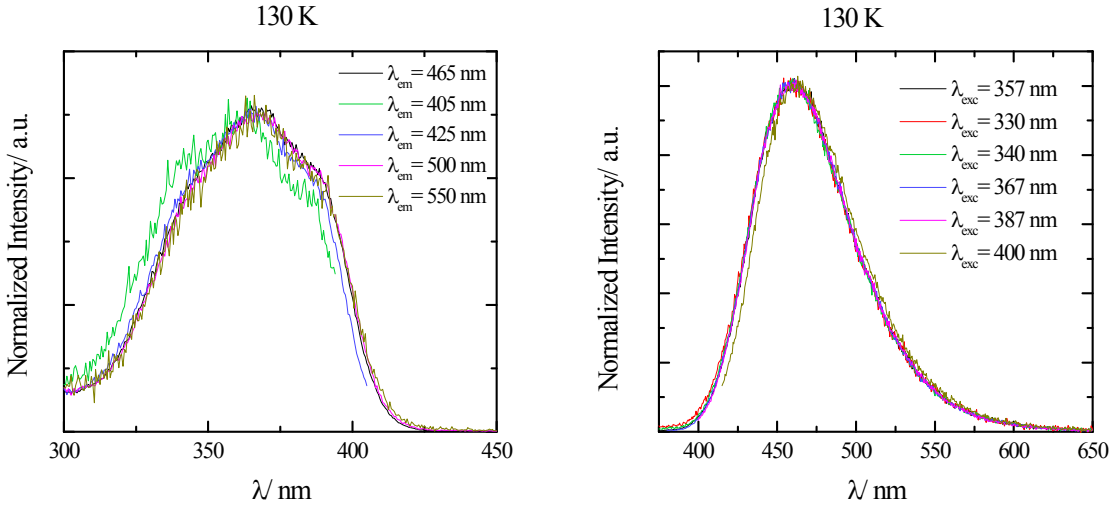

Figure 11S. Emission wavelength effect on the excitation spectrum (left graph) and excitation wavelength effect on the emission spectrum (right graph) for **2-N** in EPA at 130 K.

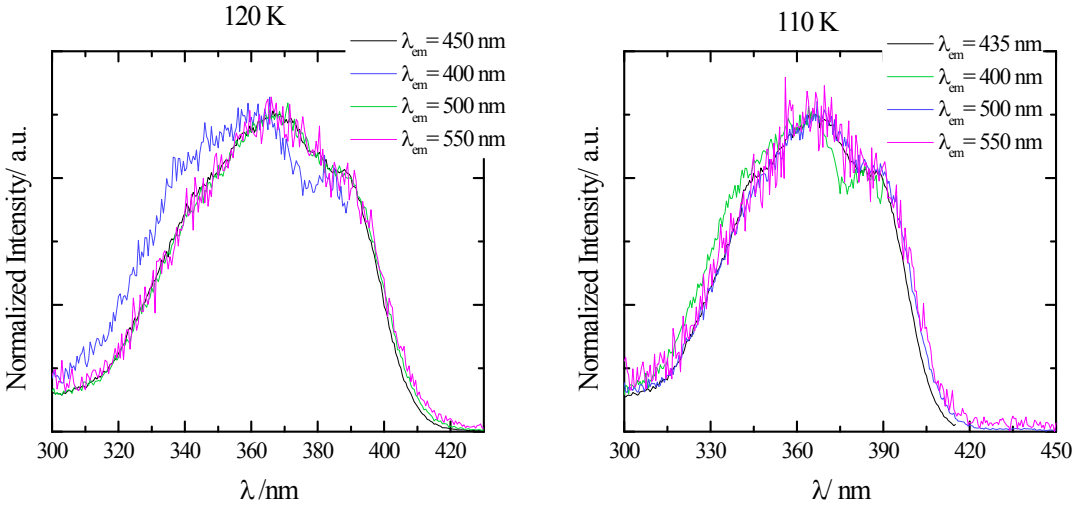

Figure 12S. Emission wavelength effect on the excitation spectrum for **2-N** in EPA at 120 K(left graph) and 110 K (right graph).

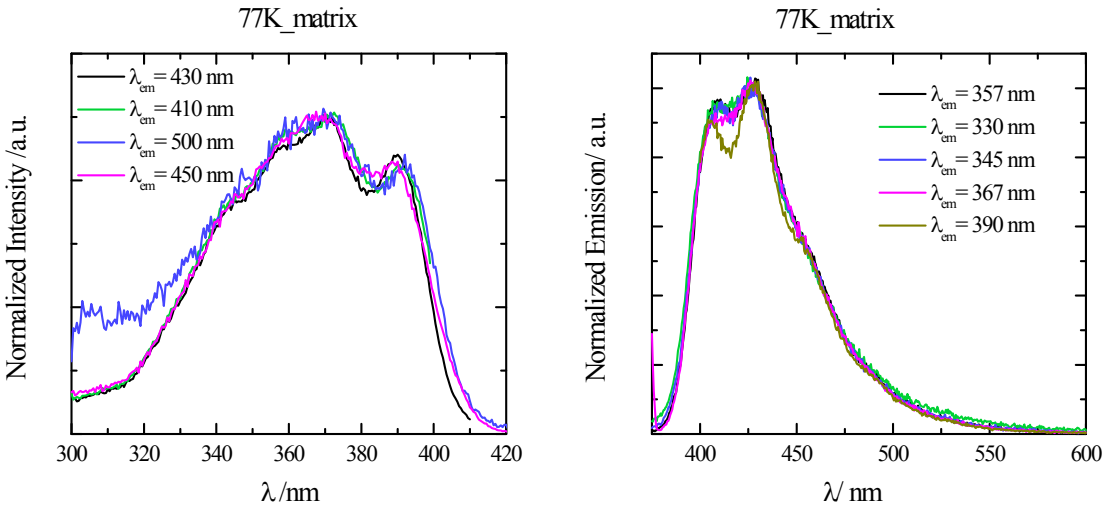

Figure 13S. Emission wavelength effect on the excitation spectrum (left graph) and excitation wavelength effect on the emission spectrum (right graph) for **2-N** in EPA matrix (77 K).

Table 4S. Wavelength effect on the fluorescence quantum yield in EPA at room temperature and in matrix at 77 K.

T = 293 K	
λ_{exc}	Φ_F
325	0.0028
340	0.0030
355	0.0033
362	0.0034
380	0.0034
400	0.0034

T = 77 K	
λ_{exc}	Φ_F
330	0.49
345	0.47
357	0.54
367	0.66
390	0.95

Table 5S. Temperature effect on the fluorescence lifetimes in EPA measured by nanosecond resolved SPC fluorescence spectroscopy (λ_{exc}=370 nm). The different colours stand for different contributions to the decay.

Temperature /K	λ_{em}					
	425 nm		480 nm		525 nm	
	τ /ns	χ^2	τ /ns	χ^2	τ /ns	χ^2
250	0.396	1.01	0.396	0.97		
220	0.788	1.03	0.769	1.02	0.644	1.12
200	0.202 1.23	1.09	0.295 1.10	0.97	 1.05	1.11
180	0.548 1.73	0.97	0.500 1.86	1.02		
160	0.827 2.66	1.00	0.800 2.66	1.00		
140	1.20 2.99	1.10	1.22 2.99	1.00		
130	0.423 1.58	0.99	- 1.64 2.99	0.98	 3.11	1.04
120	0.590 1.67	0.99	 1.76 2.83	0.97	 2.92	1.04
110	0.849 1.80	1.01	 1.80 2.90	0.99	 1.89 2.82	1.01
77	1.42 1.83	0.99	 1.81	1.03	 1.62 3.00	1.04

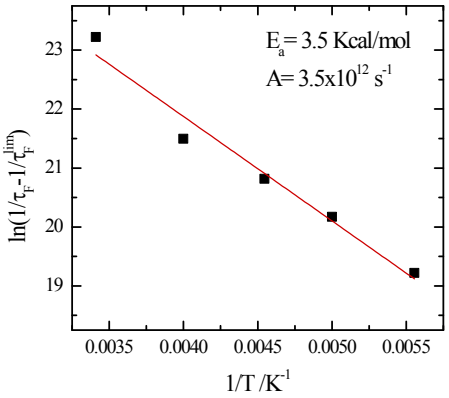

Figure 14S. Plot of the fluorescence lifetimes as a function of temperature according to the Arrhenius-type equation for the longest-living conformer.

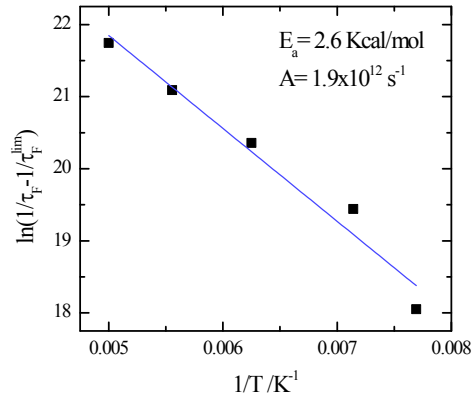

Figure 15S. Plot of the fluorescence lifetimes as a function of temperature according to the Arrhenius-type equation for the intermediate conformer.

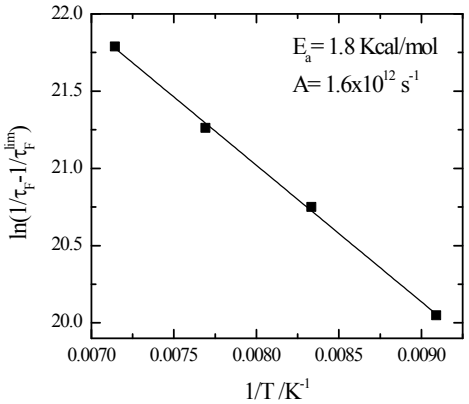

Figure 16S. Plot of the fluorescence lifetimes as a function of temperature according to the Arrhenius-type equation for the shortest conformer.